Open Access

Catalysis Research

LIDSEN Publishing Inc.

Original Research

Enhanced Photocatalytic Degradation of *p*-Nitrophenol and Phenol Red Through Synergistic Effects of a CeO_2-TiO_2 Nanocomposite

Amit Ahlawat [1, 2, †], Tarun Kumar Dhiman [2, †], Pratima R. Solanki [2], Pawan S. Rana [1, *]

1. Department of Physics, Deen Bandhu Chotu Ram University of Science and Technology, Murthal, India; E-Mails: drpawansrana.phy@dcrustm.org; drpawansrana.phy@dcrustm.org
2. Special Center for Nanoscience, Jawaharlal Nehru University, New Delhi 110067, India; E-Mails: tkdhiman91@gmail.com; partima@mail.jnu.ac.in

† These authors contributed equally to this work.

* **Correspondence:** Pawan S. Rana; E-Mail: drpawansrana.phy@dcrustm.org

Academic Editor: Ermelinda Falletta

Special Issue: Recent Advances in TiO2 Photocatalysis and Applications

Catalysis Research
2022, volume 2, issue 4
doi:10.21926/cr.2204039

Received: July 24, 2022
Accepted: October 10, 2022
Published: November 03, 2022

Abstract

Organic compounds are one of the most severe pollutants occurring in the environment. Hence, it is important to remove these compounds from the environment through remediation processes such as photocatalysis. The present study investigated the photocatalytic degradation of *p*-nitrophenol (NP) and phenol red (PR) using a cerium oxide-titanium oxide nanocomposite (CeO_2-TiO_2nc) under UV light. CeO_2-TiO_2nc was synthesized using the co-precipitation method. An X-ray diffraction (XRD) analysis confirmed the phase purity of the material. A UV-Vis absorption study revealed a broad peak in the 250–310 nm region. The photocatalytic study was performed under three irradiation conditions: no light, visible light ($\lambda > 400$ nm), and UV light ($\lambda < 400$ nm). The maximum degradation percentage for NP and PR was 97.3% and 99.8%, respectively, with the reaction rate constant (k) of 0.42 and 0.54, respectively. This is the first study to utilize the synergistic effects of TiO_2 and CeO_2 for degrading NP and PR. Over 97% degradation was achieved for both the compounds in 80

min; this result shows the high photocatalytic activity of CeO_2-TiO_2nc. Thus, CeO_2-TiO_2nc can be used as a cost-effective adsorbent with a high capacity to degrade harmful organic compounds.

Keywords
p-nitrophenol; phenol red; CeO_2; TiO_2; photocatalysis

1. Introduction

Pollutants generated from various industries are a major threat to the environment. Among these pollutants, persistent organic pollutants (POPs) are substances with critical environmental concern because of their toxicity, potential carcinogenicity, high chemical stability, and nonbiodegradability [1, 2]. Because of these characteristics, POPs are widely distributed in water bodies and remain in living beings for prolonged time periods. Wastewater from textile processing plants contains various dyes at concentrations ranging from 10 to 200 mg L^{-1}, which are carcinogenic. Some of the natural coloring dyes do not tightly bind to the surface of textile products and are released into water bodies. The amount released could vary from 2% for basic color compounds to 5% for highly reactive coloring compounds, thereby leading to severe discoloration of surface and ground waters near the coloring dye industries [3, 4]. A survey of the toxicological properties of wastewater effluents showed that coloring dye industries release highly toxic chemicals in water when compared with other industries. Some of the highly toxic chemicals released as waste materials from industries include carbon-based toxic compounds such as dibenzofurans, polychlorinated dibenzo-*p*-dioxins, and polychlorinated biphenyls and organochlorine pesticides such as dichloro-diphenyl-trichloroethane, hexachlorobenzene, dibenzo-*p*-dioxins, and dibenzo-*p*-furans [5]. These organic products are also discharged into the surrounding environment as byproducts of processes such as waste disposal and metal production.

Few organic products can also bioaccumulate and bio-magnify in the environment. Several studies have investigated various treatment methods to eliminate highly toxic compounds from water, including ozonation, precipitation, ion exchange, adsorption, advanced oxidation, and reverse osmosis; however, some of these methods are not feasible because of their high cost [6]. Coloring dyes are classified into several categories, such as acidic dyes, basic dyes, direct dyes, fluorescent dyes, sulfur dyes, reactive dyes, and precursor dyes. Currently, we are focusing on acidic dyes. Acidic dyes are water-soluble compounds with a carboxylic acid group or sulfonic acid group in their molecules. Based on chemical constituents, acidic dyes include azo compounds, triarylmethanes, anthraquinones, nitro compounds, iminoacetone, quinolines, and nitrous compounds. Azo dyes are characterized by an azo group (-N=N-) present in varying numbers. These groups are linked by phenyl and naphthyl radicals to functional groups such as chlorine, amino, hydroxyl, nitro, methyl, sodium salts, and sulfonic acid [7-9]. Consequently, azo compounds with functional groups are considered mutagenic and carcinogenic [10-12]. Several research studies have shown that the release of such compounds into the environment is alarming because their toxicity could pose a life-threatening risk to the exposed organisms. Presently,

several studies are being conducted on the degradation of organic compounds through physical processes such as flocculation; adsorption; use of silica gel, activated charcoal, and wood chips; membrane filtration, UV radiation; ion exchange technique; coagulation through electrokinetics; and filtration [13]. Chemical processes such as oxidation, Fenton reaction, ozonation, and photochemical processes are also being used for organic compound degradation [14-16]. The adsorption and membrane filtration techniques create secondary wastes that need further treatment. These challenges have led researchers to consider advanced processes and biological methods to effectively treat dye-containing wastewaters. These processes use strong oxidizing agents (Fenton process/H_2O_2) or metal oxide-based photocatalysts such as titanium dioxide (TiO_2), zinc peroxide (ZnO_2), manganese oxide/manganese dioxide (MnO/MnO_2), and ferric oxide (Fe_2O_3) in the presence of light irradiation [17-22]. Biological methods have also been used as they are environment friendly, result in the complete mineralization of organic pollutants, and involve the generation of (OH) radicals that enable the destruction of hazardous pollutants [23].

TiO_2 has been used for the photocatalytic degradation of several organic and inorganic contaminants in water. It is economical; has good stability, excellent light adsorption, and low toxicity; and can be easily recovered by filtration and centrifugation [24, 25]. However, it has a large band gap that restricts its adsorption to the UV range alone. This limitation can be overcome by doping or forming composites with different nanoparticles [26, 27]. Rare earth metals and their oxides, when combined with TiO_2, lead to a red shift by forming inter-band states [28, 29]. Their addition reduces electron-hole pair recombination by trapping the electrons in inter-bands and accelerating their mobility over TiO_2 surface [30, 31]. Cerium (Ce) shows activity in the visible light region when combined with TiO_2 [32-34]. Cerium oxide (CeO_2) is an active rare earth metal oxide with excellent stability, easily accessible due to excess quantity, nontoxicity, and economical nature [35-37]. It has been used in several different applications such as water gas shift (WGS), pollution control, oxygen sensors, solid oxide fuel cells, hydrogen generation, and wastewater treatment [38-40]. The catalytic property of CeO_2 is based on the formation of Ce^{3+} defect sites and oxygen vacancies. These defect sites reduce electron-hole pair recombination on TiO_2 surfaces, which induces higher efficiency of photocatalytic degradation in UV and visible light regions [41]. In the present study, we utilized the synergistic effects of TiO_2 and CeO_2 for degrading azo compounds.

Azo compounds are nonbiodegradable because of their extreme stability to light irradiation and resistance to microbial attack [15]. Organic compounds containing the phenolic group and its derivatives are among the common pollutants released from various industries. Among such organic compounds, *p*-nitrophenol (NP) and phenol red (PR) are the most toxic ones. They are generated from explosives, textile industries, and military establishments and can contaminate soil and water bodies. Hence, a reduction in the amount of NP and PR is very crucial because of their anthropogenic, toxic, and inhibitory characteristics. The present study aimed to conduct remediation of water polluted with NP and PR dyes by using a CeO_2-TiO_2 nanocomposite (CeO_2-TiO_2nc) through the photocatalysis process [16]. This study is the first in which synergistic effects of TiO_2 and CeO_2 were utilized for degrading NP and PR. Over 97% degradation was achieved for both the compounds in 80 min; this shows the high photocatalytic activity of CeO_2-TiO_2nc. The maximum degradation percentage for NP and PR was 97.3% and 99.8%, respectively, and the reaction rate constant (k) was 0.42 and 0.54 for NP and PR, respectively. These findings

demonstrate that CeO_2-TiO_2nc can be used as a cost-effective adsorbent with a high capacity to degrade harmful organic compounds.

2. Methods and Materials

The chemical and reagents used for synthesizing CeO_2/TiO_2nc were titanium isopropoxide (TTIP) (97%, Aldrich Chemicals), isopropanol (99%, Rankem), cerium nitrate hexahydrate (99%, Thomas Baker), and sodium hydroxide (98%, Fisher Scientific). A 100 mL solution was prepared using deionized (DI) water as the solvent. The precalculated amount, i.e., 5 mL TTIP and 10 mL isopropanol, of precursor was mixed with DI water. The gel preparation process was started following the mixing of the solutions by vigorous stirring. Hydrolysis of TTIP yielded a turbid solution that was heated at 70 °C for approximately 18–20 h. The precipitated sample was then collected and washed thrice with ethanol to neutralize the sample. This precipitate was collected and dried for 24 h at 80 °C. Finally, the prepared powder was annealed at 400 °C for 2 h. To synthesize CeO_2 nanoparticles (NPs), $Ce(NO_3)_2{\cdot}6H_2O$ was added to 100 mL DI water to prepare a 0.25 M solution. This solution was mixed under regular stirring with the as-prepared TiO_2 NPs by using the titration method. Following the complete mixing of CeO_2 and TiO_2 NPs, the solution was stirred for some time and then dried at 80 °C for 4 h. The resultant CeO_2-TiO_2nc was then calcined at 400 °C for 4 h.

The structural and optical properties of CeO_2-TiO_2nc were studied using an X-ray diffractometer (Rigaku MiniFlex) and a UV-Vis spectrometer (T90+, PG Instruments Ltd.). Solutions of NP and PR (10 ppm concentration) in 30 mL of DI water were prepared for degradation studies. Next, 30 mg of CeO_2-TiO_2nc was added to 30 mL of the NP and PR solutions separately in two beakers. The photocatalytic study of NP and PR compounds were performed under three irradiation conditions: without light, visible light ($\lambda > 400$ nm) generated through a 100 W power bulb (Philips), and UV light ($\lambda < 400$ nm) generated through a 300 W power bulb (Osram). The beaker was positioned 15 cm from the two bulbs. Next, 4 mL of sample was collected at regular intervals of 0, 20, 40, 60, and 80 min in micro centrifuge tubes. The tubes were then centrifuged (Eppendorf Centrifuge 5424R) to obtain a supernatant. UV-Vis spectra were acquired with a UV-Vis spectrometer to study the sequential degradation of NP and PR compounds. The reutilization of the catalyst was investigated by the cyclic photocatalytic study. The used catalyst was centrifuged after the first degradation study to remove the adsorbed molecules. The catalyst was then washed 4–5 times using DI water. Centrifugation was performed one more time to remove the remaining adsorbed molecules. CeO_2-TiO_2nc was further studied for 4 degradation cycles of NP and PR.

3. Results & Discussion

3.1 Characterization Results

Figure 1 shows the X-ray diffraction (XRD) spectra of CeO_2/TiO_2nc in the range of 10–70°. TiO_2 peaks are indicated by the (*) mark and are positioned at 24.91°, 37.24°, and 62.70° corresponding to (101), (004), and (204) planes, respectively. The remaining peaks in the spectra are of CeO_2 at the positions of 28.01°, 32.72°, 47.24°, 55.97°, 58.56°, and 62.70° corresponding to (111), (200), (220), (311), (222), and (400), respectively. The average crystallite size was calculated using the

Debye–Scherrer equation as explained in our previously published paper. The average crystallite size was 7.15 and 6.25 nm for TiO_2 and CeO_2, respectively [19, 42].

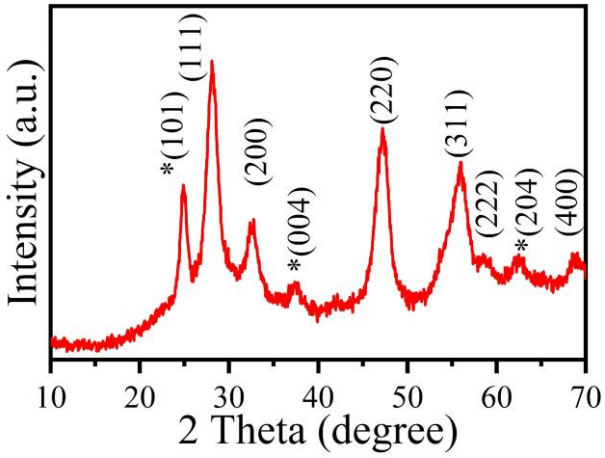

Figure 1 XRD pattern of CeO_2/TiO_2nc. The (*) mark indicates peaks obtained due to TiO_2 NPs.

Figure 2 shows the UV-Vis absorption plot for CeO_2/TiO_2nc. Two small peaks were obtained at 255 and 305 nm corresponding to TiO_2 and CeO_2, respectively. The optical band gap (E_g) was determined from the absorption profiles of CeO_2/TiO_2nc by using the Tauc plot given by

$$(\alpha h\upsilon)^2 = A(h\upsilon - E_g)$$

where α is the absorption coefficient, h is Planck's constant, n is the frequency of incident light, A is the proportionality constant, and E_g is the optical band gap. A large band gap of 3.68 eV was noted, which can allow for effective charge carrier separation and less electron–hole recombination [43, 44].

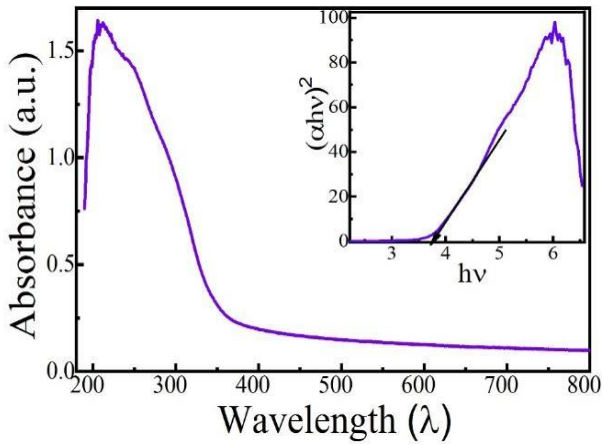

Figure 2 UV absorption of CeO_2/TiO_2nc. The inset shows Tauc's plot for calculating the band gap, which was around 3.68 eV.

Organic compounds have received considerable attention as harmful aquatic pollutants, and hence, studies are being actively conducted to develop novel remediation methods. NP and PR are azo compounds and are difficult to degrade because of their chemical properties. In the present

study, CeO_2/TiO_2nc functioned as an excellent photocatalyst under UV light and could degrade both NP and PR.

3.2 Photon-Enhanced Degradation Study of NP and PR Azo Compounds

Figure 3 displays the photocatalytic activity of CeO_2/TiO_2nc in (a) dark, (b) visible light, and (c) UV light; an excellent degradation rate of 97.3% in 80 min was achieved for NP. Figure 3 (d) shows the C/C_o plot of plot (c), which clearly indicates that the catalytic activity increased rapidly under UV light irradiation. The inset of Figure 3 (d) shows the pseudo-first-order reaction kinetic study.

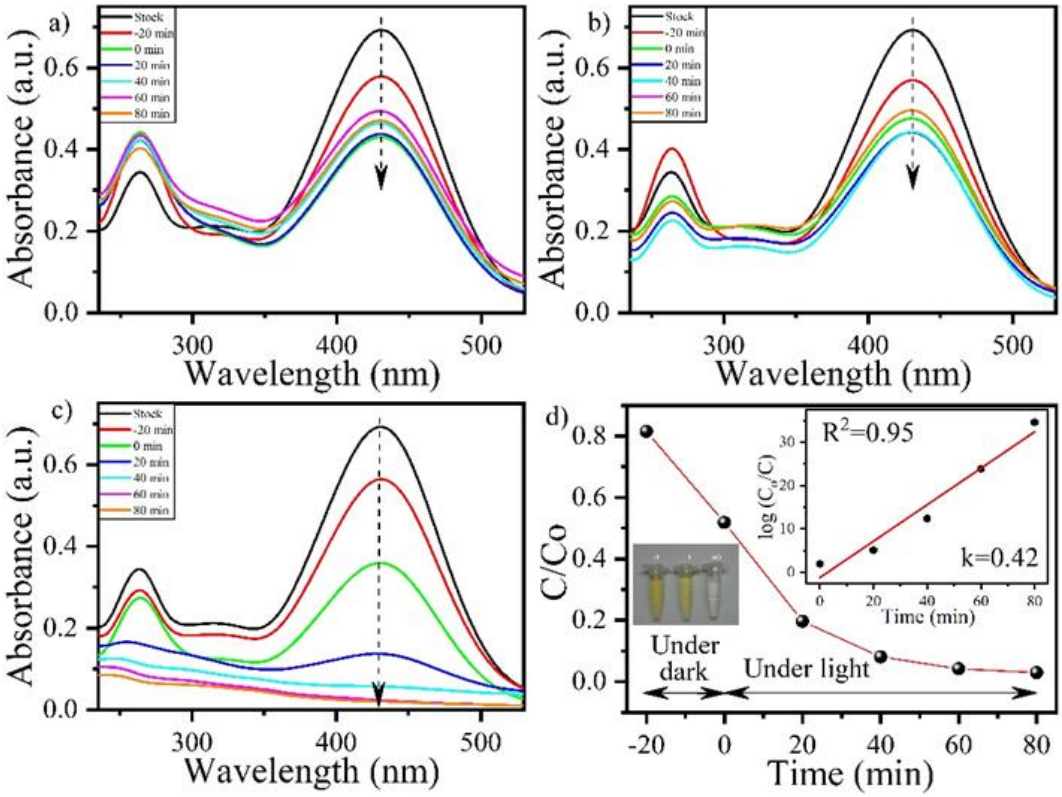

Figure 3 UV-Vis spectra of NP showing degradation studies (a) without light, (b) with visible light (λ > 400 nm), and (c) with UV light (λ < 400 nm); (d) shows a decrease in the intensity of NP with time. The inset shows the kinetic study based on pseudo-first-order for degradation studies under UV light.

Similarly, Figure 4 displays the photocatalytic activity of CeO_2/TiO_2nc in (a) dark, (b) visible light, and (c) UV light; an excellent degradation rate of 99.8% in 80 min was achieved for PR. Figure 4 (d) shows the C/C_o plot of plot (c), which clearly indicates that the catalytic activity increased rapidly under UV light irradiation. The inset of Figure 4 (d) shows the pseudo-first-order reaction kinetic study.

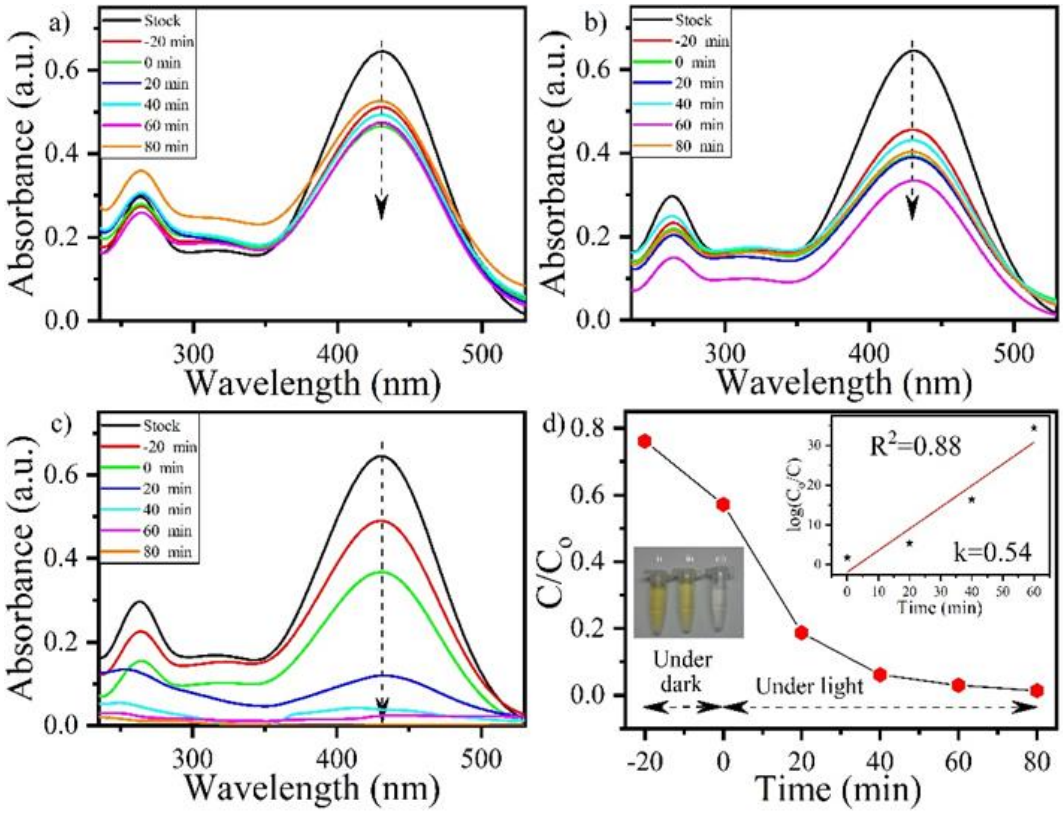

Figure 4 UV-Vis spectra of PR showing degradation studies (a) without light, (b) with visible light (λ > 400 nm), and (c) with UV light (λ < 400 nm); (d) shows a decrease in the intensity of PR with time. The inset exhibits the kinetic study based on pseudo-first-order for degradation studies under UV light.

The degradation percentages of NP and PR were calculated using the formulae

$$n = \frac{(C_i - C_f)}{C_i} \times 10$$

where c_i is the initial concentration of the dye and c_f is the final concentration of the dye. In both studies, UV-Vis spectroscopy was used to determine the initial and final concentrations of the dye, and the peak was noted at 440 nm. In dark and under visible light conditions, both NP and PR showed high intensity, while under UV light, NP and PR concentrations decreased drastically [13, 14]. In the dark, there was minimal degradation of the dyes; this was primarily because of the adsorption of NP and PR on the catalyst surface. Under visible light irradiation, no substantial difference in degradation was observed, which could be due to the larger wavelength and less energy of visible light that does not cause electron excitation to promote higher photodegradation at the surface of the nanomaterials [3, 4, 23]. However, under UV light, more than 97% degradation was achieved for both NP and PR; this finding shows that the short wavelength and high energy of UV light facilitate CeO_2/TiO_2nc in the photocatalytic degradation process.

The kinetics of the photocatalytic degradation of NP and PR and CeO_2/TiO_2nc can be expressed as follows:

$$-\left(\frac{dC}{dt}\right) = KC$$

where K is the pseudo-first-order reaction rate constant, C is the concentration of dye molecules at time t, and t is the reaction time. By integrating the above equation and taking the limits as $c = c_o$ at time t = 0, we obtain

$$ln\ ln\left(\frac{C_o}{C}\right) = Kt$$

By using the above equation, the pseudo-first-order rate constant for both the studies have been tabulated in Table 1.

Table 1 Values of R square and K for NP and PR dye degradation under UV light.

S. No.	Compound	R^2	k value (s^{-1})
1.	**NP**	0.95	0.42
2.	**PR**	0.88	0.54

3.3 Mechanisms of NP and PR Degradation

Figure 5 shows the mechanism of photocatalysis. Commonly, in semiconductors, electrons are excited from the valence band (VB) to the conduction band (CB) in the presence of light, which leads to a redox reaction [45]. In the present case, there are different band positions because of the CB and VB of CeO_2 and TiO_2. Based on the band gap, both CeO_2 and TiO_2 are considered semiconductors [46, 47]. Under irradiation with UV light, both these semiconductors are excited, which leads to the production of photogenerated electrons and holes. These photogenerated electrons are excited and reach the CB, while the photogenerated holes remain at the VB. The difference in electronegativity between CeO_2 and TiO_2 leads to a transfer of electrons from the conducting materials to the surface of NP and PR. On the surface of NP and PR, redox reactions occur, which leads to the degradation of the dye due to the generation of $OH^{\cdot}$ radicals. The electrons from the CB of the nanocomposites are responsible for the reduction process, which leads to the generation of O^{2-}, and OH° radicals, whereas the VB leads to the oxidation process and generation of OH° and OH^- radicals, which further recombine with the functional groups of azo compounds to break them into smaller harmless compounds. The mineralization process was the dominant process for the degradation of NP and PR dyes [48-50].

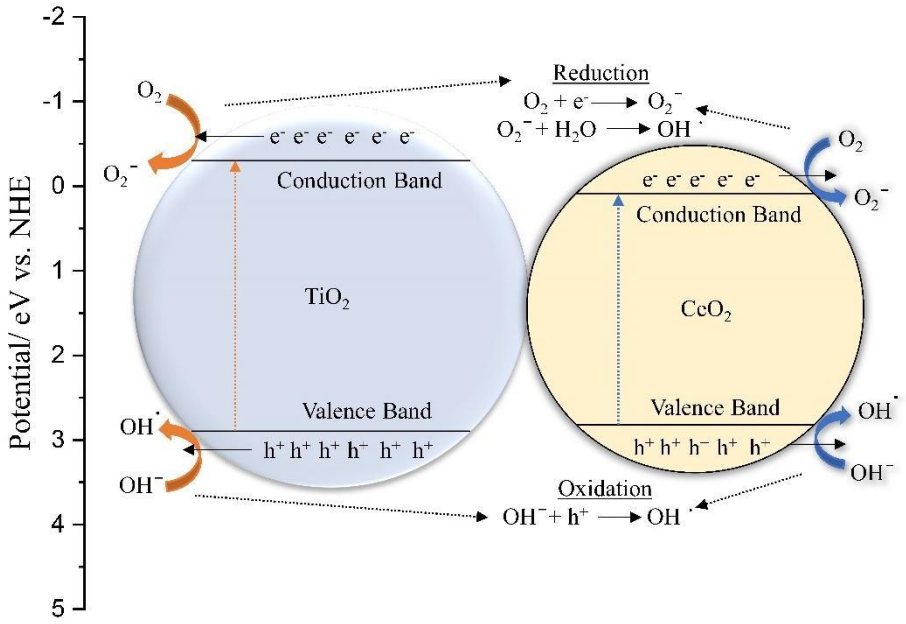

Figure 5 Oxidation and reduction mechanisms of CeO_2/TiO_2nc for generating active entities under UV light irradiation.

3.4 Cyclic Photocatalytic Study

The cyclic photodegradation study enables determining the reutilization capacity of CeO_2/TiO_2nc for multiple reuses. As shown in Figure 6, CeO_2/TiO_2nc was reused for four cycles of the photocatalytic study. The overall degradation percentage was >80% for NP and PR after four cycles of photocatalytic study.

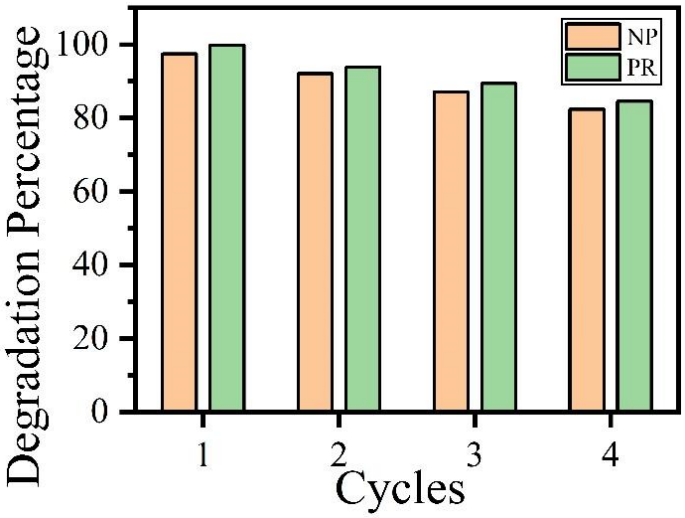

Figure 6 Cyclic photocatalytic study of CeO_2/TiO_2nc for degrading *p*-nitrophenol (NP) and phenol red (PR).

3.5 Comparison of the Current Study with Previously Reported Literature on the Degradation of NP and PR Azo Compounds

Table 2 shows the comparison of our results with the previously reported literature for NP degradation. We have chosen papers that investigated the use of TiO_2 and its composites for degrading NP.

Table 2 Comparison of the current study results with the previously reported results for *p*-nitrophenol degradation using TiO_2-based materials and composites.

S. No	Nanoparticles	Degradation Route	Degradation Time	Degradation percentage	References
1.	Zn-TCPP/Ag doped mesoporous TiO_2	Photocatalytic degradation	150	>90%	[51]
2.	Cu_2O NCs/TiO_2	Photocatalytic Degradation	240	60	[52]
3.	SiO_2/Fe_3O_4/C@TiO_2	Fenton Process	260	93	[53]
4.	TiO_2-CeO_2	Photocatalytic degradation	80	97.3	**This Work**

Table 3 shows the comparison of our results with the previously reported literature for PR degradation. Here again, we have chosen papers that investigated the use of TiO_2 and its composites for degrading PR. Compared to previous studies, by utilizing the synergistic effects of CeO_2 and TiO_2, our present study achieved higher degradation of both NP and PT in less time, along with a much simpler synthesis of the nanocomposite.

Table 3 Comparison of the current study results with the previously reported results for phenol red degradation using TiO_2-based materials and composites.

S. No.	Nanoparticles	Degradation Route	Degradation Time (min)	Degradation percentage	References
1.	Nb(x)/TiO_2 Nanocomposites	Photocatalytic Degradation	160	94%	[54]
2.	TiO_2 nanocatalyst Nitrogen-Doped	Photocatalytic discoloration	120	>90%	[55]
3.	TiO_2/WO_3 Nano-Composite	Photocatalytic Degradation	180	93.87%	[56]
4.	TiO_2 particles	Photocatalytic Degradation	300	>90%	[57]
5.	Fe/S Co-Doped Titanium Dioxide Nanotubes	Photoelectrocatalytic Degradation	706	>90%	[58]
6.	CeO_2/TiO_2nc	Photocatalytic Degradation	80	99.8%	**This work**

4. Conclusion

CeO_2/TiO_2nc was synthesized by the co-precipitation method. The XRD study confirmed the formation of a cubic structure for both CeO_2 and TiO_2, with an average crystallite size of 7.15 nm and 6.25 nm, respectively. UV-vis spectroscopy showed two distinct peaks corresponding to CeO_2 and TiO_2, with a band gap of 3.68 eV. The photocatalytic study was performed under three irradiation conditions: in the dark, under visible light, and under UV light. The maximum degradation rates for NP and PR dyes were 97.3% and 99.8% in 80 min under UV irradiation. The mineralization process was the dominant process, and the reaction rate constant was 0.42 and 0.54 for NP and PR, respectively. These results showcase that CeO_2/TiO_2nc can be used for the photocatalytic degradation of NP and PR under UV light irradiation. Compared to previously reported results, by utilizing the synergistic effects of CeO_2 and TiO_2, we achieved higher degradation rates in less time, along with a much simpler process of nanocomposite synthesis.

Acknowledgments

One of the authors, Amit Ahlawat, is thankful to UGC, India, for giving financial support through fellowship (NTA Ref No. 201610066606). The Government of India provide financial supports for this work [Indo-Russia project (DBT/IC-2/Indo-Russia/2017-19/02)]. PSR also acknowledge to DST, India for DST-FIST project (Ref. No; SR/ FST/PS-I/2012/32), sanctioned to Department of Physics, DCRUST, Murthal.

Author Contributions

Amit Ahlawat and Tarun Kumar Dhiman have performed the synthesis and characterization of the CeO2/TiO2nc and the degradation study of NP and PR. Dr. Pratima R. Solanki has helped in manuscript preparation, formatting, and mechanism of the dye degradation, Dr. Pawan S. Rana has formulated the concept of the work, calculation of the Kinetics and manuscript preparation.

Competing Interests

The authors declare no competing interests.

References

1. Burkhard LP, Lukasewycz MT. Toxicity equivalency values for polychlorinated biphenyl mixtures. Environ Toxicol Chem. 2008; 27: 529-534.
2. Fiedler H. Persistent organic pollutants. Vol. 3. Berlin/Heidelberg: Springer; 2002.
3. Jiang H, Li M, Liu J, Li X, Tian L, Chen P. Alkali-free synthesis of a novel heterostructured CeO_2-TiO_2 nanocomposite with high performance to reduce Cr(VI) under visible light. Ceram Int. 2018; 44: 2709-2717.
4. Yang H, Zhang K, Shi R, Tang A. Sol–gel synthesis and photocatalytic activity of CeO_2-TiO_2 nanocomposites. J Am Ceram Soc. 2007; 90: 1370-1374.
5. Rashed MN. Adsorption technique for the removal of organic pollutants from water and wastewater. In: Organic pollutants: Monitoring, risk and treatment. Croatia: InTech; 2013; pp. 167-194.

6. de Campos Ventura-Camargo B, Marin-Morales MA. Azo dyes: Characterization and toxicity-A review. Text Light Ind Sci Technol. 2013; 2: 85-103.
7. Idaka E, Ogawa T, Horitsu H. Reductive metabolism of aminoazobenzenes by Pseudomonas cepacia. Bull Environ Contam Toxicol. 1987; 39: 100-107.
8. Robinson T, McMullan G, Marchant R, Nigam P. Remediation of dyes in textile effluent: A critical review on current treatment technologies with a proposed alternative. Bioresour Technol. 2001; 77: 247-255.
9. Jadhav JP, Parshetti GK, Kalme SD, Govindwar SP. Decolourization of azo dye methyl red by Saccharomyces cerevisiae MTCC 463. Chemosphere. 2007; 68: 394-400.
10. Dhiman TK, Singh S. Enhanced catalytic and photocatalytic degradation of organic pollutant rhodamine-B by $LaMnO_3$ nanoparticles synthesized by non-aqueous sol-gel route. Phys Status Solidi A. 2019; 216: 1900012.
11. Ahlawat A, Rana PS, Solanki PR. Studies of photocatalytic and optoelectronic properties of microwave synthesized and polyethyleneimine stabilized carbon quantum dots. Mater Lett. 2021; 305: 130830.
12. Kujur VS, Singh S. Structural, magnetic, optical and photocatalytic properties of $GaFeO_3$ nanoparticles synthesized via non-aqueous solvent-based sol–gel route. Journal of Materials Science: Materials in Electronics. 2020; 31: 17633-17646.
13. Kujur VS, Gaur R, Gupta V, Singh S. Significantly enhanced UV-light-driven photocatalytic performance of ferroelectric $(K_{0.5}Na_{0.5})NbO_3$: Effect of corona-poling and particle size. J Phys Chem Solids. 2022; 167: 110751.
14. Levine WG. Metabolism of azo dyes: Implication for detoxication and activation. Drug Metab Rev. 1991; 23: 253-309.
15. Vandevivere PC, Bianchi R, Verstraete W. Review: Treatment and reuse of wastewater from the textile wet-processing industry: Review of emerging technologies. J Chem Technol Biotechnol. 1998; 72: 289-302.
16. Ameen S, Shaheer Akhtar M, Seo HK, Shin HS. Solution-processed CeO_2/TiO_2 nanocomposite as potent visible light photocatalyst for the degradation of bromophenol dye. Chem Eng J. 2014; 247: 193-198.
17. Dhiman TK, Ahlawat A, Solanki PR. ZnOnps based photocatalytic reactor for degradation of multiple organic pollutants driven by solar light-based UV irradiation. SPAST Abstr. 2021; 1.
18. Ahlawat A, Dhiman TK, Solanki PR. Photocatalytic degradation of gentamycin using TiO_2 nanoparticle driven by UV light irradiation. SPAST Abstr. 2021; 1.
19. Dhiman TK, Lakshmi GBVS, Kumar R, Asokan K, Solanki PR. Non-enzymatic detection of glucose using a capacitive nanobiosensor based on PVA capped CuO synthesized via co-precipitation route. IEEE Sens J. 2020; 20: 10415-10423.
20. Dhiman TK, Poddar M, Lakshmi GBVS, Kumar R, Solanki PR. Non-enzymatic and rapid detection of glucose on PVA-CuO thin film using ARDUINO UNO based capacitance measurement unit. Biomed Microdev. 2021; 23: 36.
21. Singh AK, Sri S, Garimella L, Dhiman TK, Sen S, Solanki PR. Graphene quantum dot-based optical sensing platform for aflatoxin B1 detection via the resonance energy transfer phenomenon. ACS Appl Bio Mater. 2022; 5: 1179-1186.
22. Verma AK, Ansari Z. Fluorescent ZnO quantum dot probe to study glucose–glucose oxidase interaction via fluorescence resonance energy transfer. Sens Lett. 2020; 18: 351-365.

23. Karunakaran C, Gomathisankar P. Solvothermal synthesis of CeO_2–TiO_2 nanocomposite for visible light photocatalytic detoxification of cyanide. ACS Sustain Chem Eng. 2013; 1: 1555-1563.
24. Magesh G, Viswanathan B, Viswanath R, Varadarajan T. Photocatalytic behavior of CeO_2-TiO_2 system for the degradation of methylene blue. Ind J Chem; 2009; 48A: 480-488.
25. Kansal SK, Kundu P, Sood S, Lamba R, Umar A, Mehta S. Photocatalytic degradation of the antibiotic levofloxacin using highly crystalline TiO_2 nanoparticles. New J Chem. 2014; 38: 3220-3226.
26. Bessekhouad Y, Chaoui N, Trzpit M, Ghazzal N, Robert D, Weber JV. UV–vis versus visible degradation of acid orange II in a coupled CdS/TiO_2 semiconductors suspension. J Photochem Photobiol A. 2006; 183: 218-224.
27. Wu L, Yu JC, Fu X. Characterization and photocatalytic mechanism of nanosized CdS coupled TiO_2 nanocrystals under visible light irradiation. J Mol Catal A. 2006; 244: 25-32.
28. Ho W, Yu JC. Sonochemical synthesis and visible light photocatalytic behavior of CdSe and CdSe/TiO_2 nanoparticles. J Mol Catal A. 2006; 247: 268-274.
29. Xie Y, Yuan C. Photocatalysis of neodymium ion modified TiO_2 sol under visible light irradiation. Appl Surf Sci. 2004; 221: 17-24.
30. Li FB, Li XZ, Cheah KW. Photocatalytic activity of neodymium ion doped TiO_2 for 2-mercaptobenzothiazole degradation under visible light irradiation. Environ Chem. 2005; 2: 130-137.
31. Xie Y, Yuan C. Characterization and photocatalysis of Eu^{3+}–TiO_2 sol in the hydrosol reaction system. Mater Res Bull. 2004; 39: 533-543.
32. Xie Y, Yuan C, Li X. Photosensitized and photocatalyzed degradation of azo dye using Ln^{n+}-TiO_2 sol in aqueous solution under visible light irradiation. Mater Sci Eng B. 2005; 117: 325-333.
33. Tong T, Zhang J, Tian B, Chen F, He D, Anpo M. Preparation of Ce-TiO_2 catalysts by controlled hydrolysis of titanium alkoxide based on esterification reaction and study on its photocatalytic activity. J Colloid Interface Sci. 2007; 315: 382-388.
34. Pavasupree S, Suzuki Y, Pivsa-Art S, Yoshikawa S. Preparation and characterization of mesoporous CeO_2–TiO_2 nanopowders respond to visible wavelength. J Solid State Chem. 2005; 178: 128-134.
35. Liu B, Zhao X, Zhang N, Zhao Q, He X, Feng J. Photocatalytic mechanism of TiO_2–CeO_2 films prepared by magnetron sputtering under UV and visible light. Surf Sci. 2005; 595: 203-211.
36. Zhang G, Ao J, Guo Y, Zhang Z, Shao M, Wang L, et al. Green synthesis and catalytic performance of nanoscale CeO_2 sheets. RSC Adv. 2014; 4: 20131-20135.
37. Padervand M, Heidarpour H, Goshadehzehn M, Hajiahmadi S. Photocatalytic degradation of 3-methyl-4-nitrophenol over Ag/AgCl-decorated/[MOYI]-coated/ZnO nanostructures: Material characterization, photocatalytic performance, and in-vivo toxicity assessment of the photoproducts. Environ Technol Innov. 2021; 21: 101212.
38. Padervand M, Lammel G, Bargahi A, Mohammad-Shiri H. Photochemical degradation of the environmental pollutants over the worm-like Nd_2CuO_4-Nd_2O_3 nanostructures. Nano-Struct Nano-Objects. 2019; 18: 100258.
39. Haneda M, Kaneko T, Kamiuchi N, Ozawa M. Improved three-way catalytic activity of bimetallic Ir–Rh catalysts supported on CeO_2–ZrO_2. Catal Sci Technol. 2015; 5: 1792-1800.

40. Liu M, Wang S, Chen T, Yuan C, Zhou Y, Wang S, et al. Performance of the nano-structured Cu–Ni (alloy) -CeO_2 anode for solid oxide fuel cells. J Power Sour. 2015; 274: 730-735.
41. Lakshmi GB, Poddar M, Dhiman TK, Singh AK, Solanki PR. Gold-Ceria nanocomposite based highly sensitive and selective aptasensing platform for the detection of the Chlorpyrifos in Solanum tuberosum. Colloids Surf A. 2022; 653: 129819.
42. Singh AK, Dhiman TK, Lakshmi G, Raj R, Jha SK, Solanki PR. Rapid and label-free detection of aflatoxin-B1viamicrofluidic electrochemical biosensor based on manganese (III) oxide (Mn_3O_4) synthesized by co-precipitation route at room temperature. Nanotechnology. 2022; 33: 285501.
43. Kumar R, Lakshmi GBVS, Dhiman TK, Singh K, Solanki PR. Highly sensitive amoxicillin immunosensor based on aqueous vanadium disulphide quantum dots. J Electroanal Chem. 2021; 892: 115266.
44. Kumar R, Singh AK, Dhiman TK, Lakshmi GBVS, Solanki PR, Singh K. Transition metal dichalcogenide quantum dots based optical detection platform for Cu^{2+} ions in water. SPAST Abstr. 2021; 1.
45. Prajapati PK, Singh H, Yadav R, Sinha AK, Szunerits S, Boukherroub R, et al. Core-shell Ni/NiO grafted cobalt (II) complex: An efficient inorganic nanocomposite for photocatalytic reduction of CO_2 under visible light irradiation. Appl Surf Sci. 2019; 467-468: 370-381.
46. Padervand M, Ghasemi S, Hajiahmadi S, Rhimi B, Nejad ZG, Karima S, et al. Multifunctional Ag/AgCl/$ZnTiO_3$ structures as highly efficient photocatalysts for the removal of nitrophenols, CO_2 photoreduction, biomedical waste treatment, and bacteria inactivation. Appl Catal A. 2022; 643: 118794.
47. Pudukudy M, Jia Q, Yuan J, Megala S, Rajendran R, Shan S. Influence of CeO_2 loading on the structural, textural, optical and photocatalytic properties of single-pot sol-gel derived ultrafine CeO_2/TiO_2 nanocomposites for the efficient degradation of tetracycline under visible light irradiation. Mater Sci Semicond Process. 2020; 108: 104891.
48. Lu C, Yin Z, Sun C, Chen C, Wang F. Photocatalytic reduction of nitroaromatics into anilines using CeO_2-TiO_2 nanocomposite. Mol Catal. 2021; 513: 111775.
49. Ahlawat A, Dhiman TK, Rana PS, Solanki PR. CeO_2/TiO_2 based nano composite for photocatalytic degradation of azo-dyes: Nitrophenol and phenol red. SPAST Abstr. 2021; 1.
50. Singh AK, Ahlawat A, Dhiman TK, Lakshmi GBVS, Solanki PR. Degradation of methyl parathion using manganese oxide (MnO_2) nanoparticles through photocatalysis. SPAST Abstr. 2021; 1.
51. Rabbani M, Bathaee H, Rahimi R, Maleki A. Photocatalytic degradation of p-nitrophenol and methylene blue using Zn-TCPP/Ag doped mesoporous TiO_2 under UV and visible light irradiation. Desalination Water Treat. 2016; 57: 25848-25856.
52. Lu Y, Xu Y, Wu Q, Yu H, Zhao Y, Qu J, et al. Synthesis of Cu_2O nanocrystals/TiO_2 photonic crystal composite for efficient p-nitrophenol removal. Colloids Surf A. 2018; 539: 291-300.
53. Hou Y, Wang Y, Yuan H, Chen H, Chen G, Shen J, et al. The enhanced catalytic degradation of SiO_2/Fe_3O_4/C@TiO_2 photo-fenton system on p-nitrophenol. J Nanopart Res. 2016; 18: 343.
54. Almulhem N, Awada C, Shaalan NM. Photocatalytic degradation of phenol red in water on Nb(x)/TiO_2 nanocomposites. Crystals. 2022; 12: 911.
55. Sagharigar T, Baniasadi B, Ebadi M, Asri M, Aliabadi M. Photocatalytic discoloration of aqueous phenol red solutions using TiO_2 nanocatalyst. J Biodivers Environ Sci. 2014; 5: 336-342.

56. Hagos TT. Synthesis and characterization of nitrogen-doped TiO_2/WO_3 nano-composite material and its photocatalytic activity for photo-degradation of phenol red in aqueous solution. Int J Innov Sci Res. 2014; 9: 357-362.
57. Wahab HS, Hussain AA. Photocatalytic oxidation of phenol red onto nanocrystalline TiO_2 particles. J Nanostruct Chem. 2016; 6: 261-274.
58. Lopez ECR, Saputil NEB, Loza LA, Camiguing FFG, Mopon Jr ML, Perez JVD. Fe/S co-doped titanium dioxide nanotubes: Optimization of the photoelectrocatalytic degradation kinetics of phenol red. Key Eng Mater; 2021; 891: 49-55.